

PACS 73.20.Mf

New features of surface plasmon resonance detected by modulation of electromagnetic radiation polarization

L.J. Berezhinsky, I.E. Matyash, S.P. Rudenko, B.K. Serdega

V. Lashkaryov Institute of Semiconductor Physics, NAS of Ukraine

45, prospect Nauky, 03028 Kyiv, Ukraine

Phone: (380-44) 525-57-78; e-mail: serdega@isp.kiev.ua

Abstract. Using a technique based on modulation of electromagnetic radiation polarization, we studied the features of surface plasmon resonance in gold nanofilms deposited onto the surface of a totally reflecting prism (fused quartz). The angular characteristics of the polarization difference of squares of the reflectance coefficient modules for *s*- and *p*-polarized radiation, $\Delta\rho = |R_s|^2 - |R_p|^2$, were measured (at a wavelength $\lambda = 0.63 \mu\text{m}$) for metal films whose thickness varied from 0 up to 120 nm. Contrary to the results given by the traditional techniques, the characteristics of $\Delta\rho$ peak under the resonance condition. As a result, two nonresonance components were found in these characteristics. The values and shapes of their angular dependences are determined by the coefficients of internal reflection from the metal and insulator that depend on the film thickness. Application of a model with exponential dependence of the refraction and extinction coefficients on the metal film thickness led to agreement between the results of calculation from the Fresnel formulas and those obtained experimentally. It was found that characteristic parameter of the exponential corresponds to the metal film thickness value of $11 \pm 0.5 \text{ nm}$.

Keywords: surface plasmon resonance, polarization modulation, dichroism.

Manuscript received 17.01.08; accepted for publication 07.02.08; published online 31.03.08.

1. Introduction

Here we consider concurrently the electromagnetic radiation polarization modulation (PM) technique and the effect of surface plasmon resonance (SPR). Such an approach has its justification. To illustrate this, let us refer to the existing classification of polarization effects [1]. According to it, the effect of internal reflection may be characterized by linear amplitude and phase anisotropies. One of these characteristics, namely, amplitude anisotropy may be exemplified by the effect of dichroism. It consists in dependence of the coefficient of absorption (reflection) of linear polarized radiation on the polarization azimuth (an angle between the electric field vector and plane of incidence of the electromagnetic wave) relative to the optical axis of an anisotropic sample. [2]. SPR is a polarization effect observed at internal reflection, so it also demonstrates dichroism.

The SPR effect consists in interaction of external radiation (whose momentum has to fulfill certain

requirements) with the charge density waves propagating along a surface or interface. The effect has been studied for two to three decades, but it still attracts attention of experimentalists [3]. There are several reasons for this. One of them is a great variety of the features of macroscopic waves that are excited near an interface between two media with different dielectric properties. Besides, the SPR effect is of some practical significance, which permanently finds new application areas [4]. The properties of the waves, conditions of their appearance and manifestation are considered in several monographs (see, e.g., [5, 6]), and the main techniques used for their investigation are presented in [7, 8]. While differing in details, these two techniques have a common feature: in both the dependence of the coefficient of internal reflection from a prism (semicylinder) surface on the angle of incidence is measured (the so-called Kretschmann and Otto geometries). The probe radiation should be linear polarized, and the electric field vector should be parallel to the plane of light incidence (*p*-polarization). The most popular technique for effect

detection involves measurement of the dependence of the reflection coefficient for radiation of the same polarization on the angle of incidence. The minimal amplitude value in the above dependence indicates a resonance.

Another reason for PM technique application when studying SPR is not so much absence of publications on the issue as its considerable information efficiency. Earlier we have demonstrated the advantage of the PM technique application for studies of the dichroism [9] and photopleochroism [10] effects. In the course of development of the differential spectroscopy [11], the PM technique (which was one of its branches) has not got adequate attention from the experimentalists. Contrary to the all known versions of modulation spectroscopy method, modulation of polarization as spatial characteristic of electromagnetic radiation is realized by two-dimensional action on electromagnetic wave. This fact (although being insignificant *prima facie*) makes experimental technique more complicated, as well as needs development of a novel interpretation of the results obtained. Earlier we have demonstrated one of the versions of such interpretation when studying linear dichroism [12]. In that case, it was found (when measuring the effects of amplitude anisotropy, i.e., a difference between transparency and reflection) that the PM technique is in essence physical differentiation of a function measured with respect to the light absorption coefficient. To ensure usability of this feature of the PM technique, anisotropy of the object under investigation has to be low. The effect of internal reflection does not meet this requirement because it is characterized by high amplitude anisotropy, especially at light incidence at an angle close to the Brewster's one. However, the features of differentiation in the course of measurement of reflection with PM still remain in this case. To detect plasmon resonance using the PM technique, one measures $\Delta\rho = \rho_s - \rho_p$, i.e., polarization difference of

the reflection coefficients $\rho_s = |R_s|^2$ and $\rho_p = |R_p|^2$ for *s*- and *p*-polarized radiation. That is why the discriminative features of the two characteristics, $|R_s|^2 = f_s(\phi)$ and $|R_p|^2 = f_p(\phi)$, are pronounced more clearly in the result obtained in the form $\Delta\rho = f(\phi)$. In this case, one may expect that those SPR features that are not detected with the traditional technique will become observable.

2. Formalism

In the simplest case, the SPR effect is observed when radiation is propagating through a medium that involves (at least) three layers. The first of them (glass) should be denser than the air. The second one (with thickness d) is a metal or heavily doped semiconductor with a complex refractive index $N_1 = n + i\chi$. The third layer is usually

the air. To consider the effect as a version of the general reflection phenomenon, the formalism of Fresnel equations is used [13]. In this case, evolution of radiation polarization states in the course of passing the layers and reflection at their boundaries is presented in the matrix form. The product of matrices in the light passage sequence enables one to present the state of radiation in the final form as $M_p = I_{p01}L_1I_{p12}$, where

$$L_1 = \begin{vmatrix} \exp(-I\beta) & 0 \\ 0 & \exp(I\beta) \end{vmatrix}, \quad I_{p01} = \begin{vmatrix} 1 & r_{p01} \\ r_{p01} & 1 \end{vmatrix},$$

$$I_{p12} = \begin{vmatrix} 1 & r_{p12} \\ r_{p12} & 1 \end{vmatrix}, \quad r_{p01} = \frac{N_1 \cos \phi_0 - N_0 \cos \phi_1}{N_1 \cos \phi_0 + N_0 \cos \phi_1} \quad \text{and}$$

$$r_{p12} = \frac{N_2 \cos \phi_1 - N_1 \cos \phi_2}{N_2 \cos \phi_1 + N_1 \cos \phi_2}. \quad \text{Here } \phi_0 \text{ is the angle of}$$

light incidence; $\phi_1 = \arcsin\left(\frac{N_0 \sin \phi_0}{N_1}\right)$;

$\phi_2 = \arcsin\left(\frac{N_0 \sin \phi_0}{N_2}\right)$; N_0 , N_1 and N_2 are the refractive

indices of the prism, film and ambient (air), respectively. (In the case of *s*-polarization, the subscript *p* should be replaced with *s*.) The phase factor

$$\beta = \frac{2\pi d \sqrt{(N_1^2 - N_0^2 \sin^2 \phi_0)^2}}{\lambda} \quad \text{is common for both}$$

polarizations.

The above expressions make it possible to determine the Fresnel reflection coefficients for electromagnetic waves of both polarizations:

$$R_p = \frac{M_{p(2,1)}}{M_{p(1,1)}}, \quad R_s = \frac{M_{s(2,1)}}{M_{s(1,1)}}. \quad (1)$$

Here $M_{p(2,1)}$, $M_{p(1,1)}$, $M_{s(2,1)}$ and $M_{s(1,1)}$ are the corresponding matrix elements for *p*- and *s*-polarization, respectively. It follows from Eq. (1) that the quantity measured is

$$\Delta\rho = \left(|R_s|^2 - |R_p|^2 \right). \quad (2)$$

3. Experimental procedure

Shown in Fig. 1 is a version of the optical schematic where PM is applied, in accordance with [14], for measurement of both internal reflection characteristics and polarization difference $\Delta\rho$ of the reflection coefficients for *s*- and *p*-polarized radiation. A He-Ne laser LHN-113 serves as radiation source (wavelength $\lambda = 0.63 \mu\text{m}$). The following two further versions are possible. In one of them, the azimuth of linear polarization is set at an angle of 0 or 90° relative to the plane of incidence. A photoelastic modulator of polarization PEM [15] is functioning as a dynamic half-wave

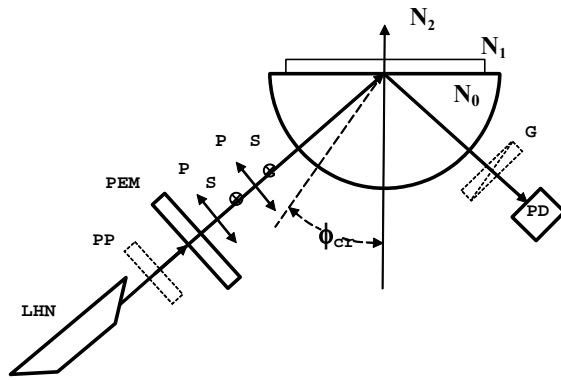


Fig. 1. Optical schematic of the experimental setup for measurement of angular characteristics of the polarization difference $\Delta\rho$ by applying polarization modulation. LHN – a He-Ne laser; PP – a quarter-wave phase plate; PEM – photoelastic modulator of polarization; P, S – linear polarizations whose azimuths are, respectively, parallel and perpendicular to the plane of incidence; G – a Glan prism; PD – a photodetector; ϕ_{cr} – the critical TIR angle; N_0 , N_1 and N_2 – the refractive indices of glass, metal and air, respectively.

plate. It transforms the wave polarization in such a way that during the period the electric field azimuth twice changes its position, from parallel to perpendicular relative to the plane of light incidence. After interaction with the prism (fused quartz) or a resonance-sensitive film on its working face, the radiation is sent to a photodetector PD (silicon photodiode). The radiation absorbed by PD generates a signal whose alternating component (at a frequency 2ω of the resonator part of modulator) is proportional to the difference of the reflection coefficients for p - and s -polarizations.

In another version, circular polarized radiation (obtained from linear polarized one with a quarter-wave phase plate PP) is sent to the modulator. The operating mode of the modulator is set by its power supply as that of a dynamic quarter-wave plate. In this case, radiation which has passed through it becomes linear polarized, and its azimuth changes by 90° during a period of modulation. The azimuth is related to the axes of the modulator phase plate (angle of 45°), so one can (by rotating about the optical axis) set such its position at which the polarization azimuths take in turn parallel and perpendicular position relative to the plane of incidence (p - and s -polarizations, respectively). In this case, the photodetector generates an alternating signal component (at a resonator frequency ω) that is also proportional to the difference of reflection coefficients. This version of SPR parameters measurement has some advantages over the former one, namely, more acceptable mode of modulator power supply and possibility to use slower-acting (i.e., more sensitive) photodetector.

After having passed through the modulator, radiation is sent to a total internal reflection (TIR) semicylinder, with a gold layer of certain thickness

deposited onto its working surface. The reflection coefficients R_p and R_s for p - and s -polarized radiation are different, so a signal from the photodetector PD (which is measured with a selective voltmeter at a modulation frequency) is proportional to the difference of the squares of the corresponding coefficient modules:

$$\Delta I \approx \left(|R_s|^2 - |R_p|^2 \right) \sin \omega t.$$

In the same version, presence of a linear polarizer G before the photodetector results in intensity modulation for that polarization relative to which the polarizer is transmission-oriented. By measuring this intensity, one can obtain the SPR characteristic in its traditional form, i.e., as a narrow angular dependence of the reflection coefficient for p -polarization only, $\rho_p = |R_p|^2$, whose amplitude becomes minimal at resonance excitation.

We took the SPR angular dependences ($\Delta\rho$, as well as ρ_s and ρ_p separately) for the samples with gold (Au – 99.999%) films whose thickness d varied in the 5–200 nm range. The films were thermally evaporated from a molybdenum heater in the vacuum (pressure of 1×10^{-3} Pa) onto a substrate at room temperature. The gold deposition rate was 1.0–1.5 nm/s; by varying time of evaporation, it was possible to obtain the required film thickness in the 5–200 nm range. The film topology, as well as more accurate measurement of film thickness (when surface nonuniformity at a level of 5 nm was taken into account by averaging), was performed with atomic force microscopy. Thin (1 mm) glass plates served as substrates. With their free surface being in contact with immersion liquid (glycerol), they made a semicylinder with the glass segment. Thus multiple changes of the samples under investigation ensured reproducibility of the semicylinder position relative light beam (and consequently of the angle reading).

4. Results and discussion

First of all, let us remind that when a prism with a resonance-sensitive film is angular-scanned with a p -polarized beam, then the result of measurement is a curve characterized by the minimal value of reflection coefficient ρ_p under the resonance condition when $\phi = \phi_{min}$ [16]. If the same scanning is performed at polarization modulation, then the result of measurement is a curve $\Delta\rho$ presenting differences of the ordinates of ρ_s and ρ_p curves (that are practically concurrently measured separately with our technique). Fig. 2 presents all the three characteristics for one of the samples under investigation (with $d = 50$ nm). One can see that the signal amplitude $\Delta\rho$ peaks at the angle ϕ_{min} . It should be noted that permutation of terms in Eq. (2) affects the signal sign only which is of no importance at synchronous-phase detection. As to the signal peak value, it remains unchanged because in every case it is counted off from one of the curves (ρ_s or ρ_p) that serves as

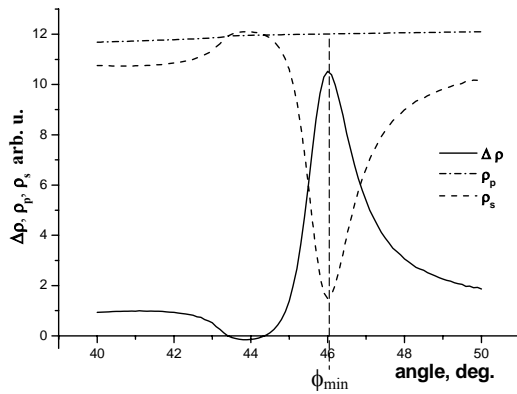


Fig. 2. The reflection coefficients ρ_s и ρ_p for s - and p -polarized radiation and their difference $\Delta\rho$ as function of the angle of light incidence ϕ_0 for a sample with $d = 50$ nm.

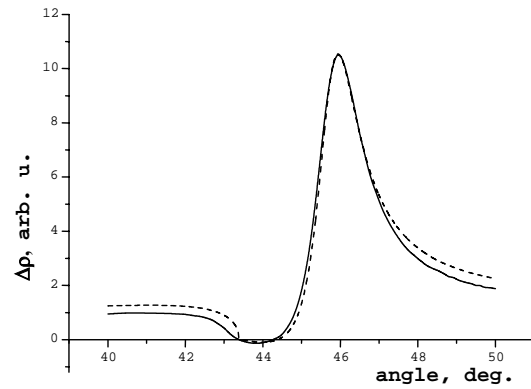


Fig. 3. The calculated (broken curve) and experimental (full curve) dependences of $\Delta\rho$ on the angle of light incidence ϕ_0 for a sample with $d = 50$ nm. The following values were used in the calculation: $L = 11$ nm; $\lambda = 630$ nm; $N_0 = 1.4742$; $N_1 = 0.2 + \exp(-0.2 - d/L)$; $\chi_1 = 3.6(1 - \exp(-d/L))$.

abscissa axis in such measuring technique. One can see also from Fig. 2 that the curves ρ_p and $\Delta\rho$ cannot be symmetric relative to some horizontal axis due to curve ρ_s dispersion near the resonance angle. The dispersion is pronounced more strongly as the film thickness decreases; this will be discussed below.

Both experimental and calculated (from Eq. (2)) characteristics of the polarization difference $\Delta\rho$ obtained for the same sample are presented in Fig. 3. The agreement between them is excellent (even in the region of negative values). Largely this results from the chosen model for dependence of optical properties of the film on its thickness. The following functions were used for this dependence:

$$n_1 = 0.2 + \exp(-0.2 - d/L); \chi_1 = 3.6 \times [1 - \exp(-d/L)]. \quad (3)$$

The characteristic length L (determined from the best possible fit of the calculated data to the experimental ones) is $L = 11 \pm 0.5$ nm for the wavelength $\lambda = 0.632$ μm . The values of the optical constants n_1 and χ_1 were taken to be those of vacuum (at the outer film surface) and those of bulk material (at another film surface). Their values are given in [17]; for the wavelength used in our work, they are $n_1 = 0.2$ and $\chi_1 = 3.6$.

To interpret the negative $\Delta\rho$ value near the angle $\phi_0 = 44^\circ$ (see Fig. 3), we apply the angular dependences of all the three quantities ρ_s , ρ_p and $\Delta\rho$ measured on one of the thinnest samples used. To explain the distinguisher feature, we present separately in Fig. 4a the angular characteristics of the coefficients of reflection of s - and p -polarized radiation from the prism surface with a gold film 5 nm thick. One can see that the characteristics for ρ of s - and p -polarizations intersect near the Brewster's angle $\phi_0 < \phi_{cr}$ due to violation of TIR conditions by the metal film. Just this fact is the reason for appearance of negative sign in the characteristic of the polarization difference $\Delta\rho$. This

conclusion is supported by Fig. 4b demonstrating agreement between the $\Delta\rho$ value obtained by geometric subtraction of curves in Fig. 4a and the results of calculation made with allowance for model dependence of dielectric properties of the film on its thickness – see Eq. (3). It was found experimentally that both the polarization difference amplitude and the angle range where polarization difference is negative depend on the film thickness. The lower boundary of this range is close to the critical angle $\phi_{cr} = 43^\circ$ corresponding to the amplitude extremum at $d = 5$ nm, while the upper bound reaches (as film thickness decreases) the value corresponding to light beam propagation along the film surface (when the grazing angle is zero). One can conclude from Fig. 4 that, as the metal film thickness decreases, the angular dependence of $\Delta\rho$ is transforming gradually from that characteristic of metal at prism surface to the characteristic of TIR violated by the ambience where the dielectric properties are determined by a film of variable thickness.

Evolution of angular dependences of SPR (due to variation of metal film nature or thickness, or dielectric properties of ambience) measured with the traditional technique has been studied rather well (see, e.g., [16]). However, the form of characteristics of the polarization difference $\Delta\rho$ differs essentially from the known ones. This fact encourages one to reconsider the effect of sample thickness on evolution of PM dependences. To this end, we measured $\Delta\rho$ values for samples of different thicknesses d (nm): 0, 5, 23, 35, 50, 90, 120, and 200. The results presented in Fig. 5a are more convenient for visual analysis when being compared with the corresponding theoretical dependences. The ground for such comparison is the agreement between the calculated and experimental results in Fig. 3. A set of $\Delta\rho$ curves calculated from Eq. (2) is presented in Fig. 5b for the angle range 40–50° near the plasmon resonance and the film thickness range from 0 up to 100 nm.

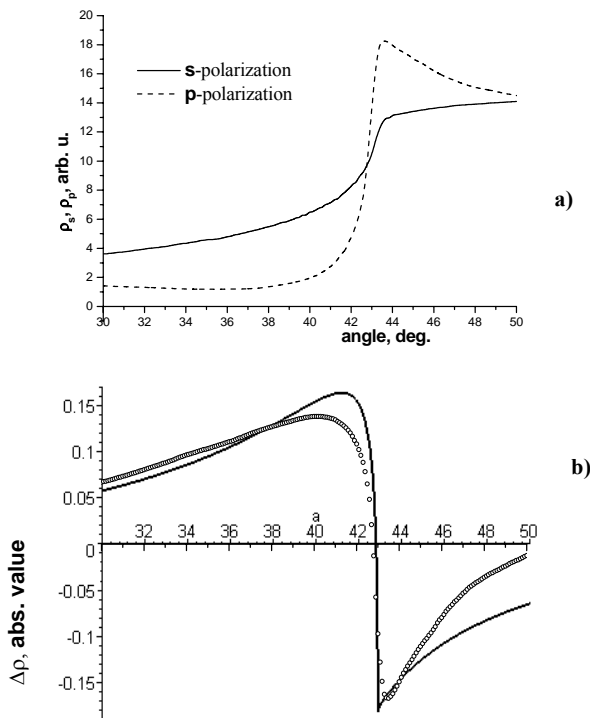


Fig. 4. a) The experimental angular dependences of ρ_s and ρ_p for a sample with $d = 5$ nm; b) the angular dependence of $\Delta\rho$ obtained by geometric subtraction of curves in Fig. 4a (dots) and calculated dependence (full curve) obtained from Eq. (2) at the following parameter values: $n_0 = 1.4742$; $n_2 = 1.003$; $N_1 = n_1 + i\chi_1$; $n_1 = 0.2 + \exp(-0.2 - d/L)$; $\chi_1 = 3.6(1 - \exp(-d/L))$; $L = 11$ nm.

Let us note some characteristic properties of the above set. Two of them are related to the positive extrema of the parameter $\Delta\rho$ which are located on either side of the critical angle $\phi_{cr} = 43^\circ$. The form of the characteristics at $\phi_0 < \phi_{cr}$ is determined by the properties of attenuated internal reflection. The set of extrema located in a small angle range at $\phi_0 \cong 46^\circ$ illustrates resonance interaction of radiation with surface plasmons. The third feature of the given set of dependences is that some of them are negative, with an extremum at $\phi_0 > \phi_{cr}$, and their amplitudes depend on sample thickness non-monotonically. One can see that comparison between Figs. 5a and 5b demonstrates a qualitative agreement between the sets (each of them has the same three characteristic properties). As to quantitative agreement, it was shown earlier that each of the experimental curves in Fig. 5a might be correlated with the corresponding dependence in Fig. 5b.

An analysis of Eq. (2) which describes the effect showed that both the negative value of the polarization difference $\Delta\rho$ and its distribution presented in the coordinates angle–thickness depend, to a great extent, on how the metal film permittivity depends on the film thickness. This is illustrated by Fig. 6 where the dependences of the polarization difference $\Delta\rho$ on the thickness of metal film at the TIR prism surface are

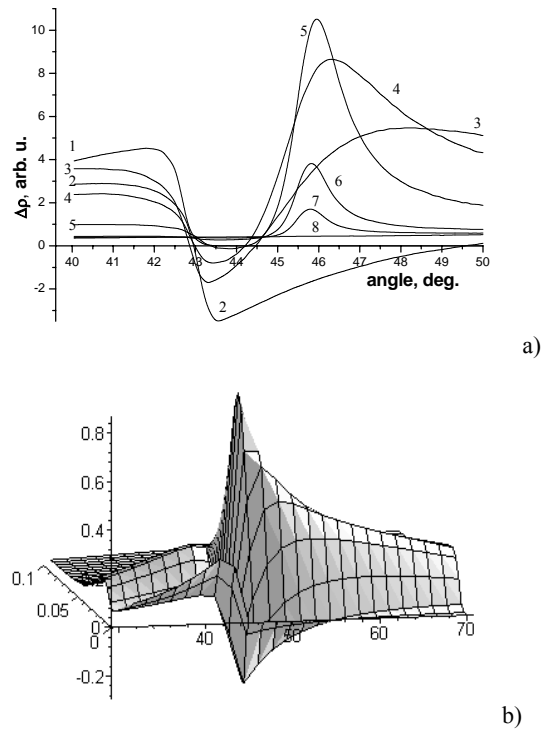


Fig. 5. a) The polarization difference $\Delta\rho$ (in the coordinates ϕ_0-d) for samples with d (nm) = 0 (1); 5(2); 23(3); 35(4); 50(5); 90(6); 120(7); and 200(8); b) the calculated polarization difference $\Delta\rho$ (in the coordinates ϕ_0-d) obtained from Eq. (2).

presented on a section of the marked coordinate area with the plane $\phi_0 = 42^\circ < \phi_{cr}$. Here the dots A correspond to the experimental values, while B (C) give the results of calculations made with (without) allowance for optical constants dependence on the film thickness. When calculating the curve B , we used the dependences of the real and imaginary parts of the film refractive index on the film thickness d given by Eq. (3), with the characteristic length $L = 11$ nm. Applicability of such extrapolation is supported by a more than satisfactory agreement between the experimental data and those calculated in the version B . As to the physical meaning of the parameter L , one may interpret it as a thickness: as it grows, the film takes on the properties of bulk material. That is, electromagnetic interaction between the wave and plasma that is characterized with a set of parameters (one of which is the electron path length in a field) becomes independent of thickness.

One more feature of the SPR characteristics measured with the PM technique is related to appearance of traditional reflection from metal in them. This is pronounced more clearly in rather thick films where the angular dependence of $\Delta\rho$ is not distorted with resonance. The corresponding curve calculated from Eq. (2) is presented in Fig. 7 for a sample with $d = 90$ nm. The form of the curve is rather simple. It is

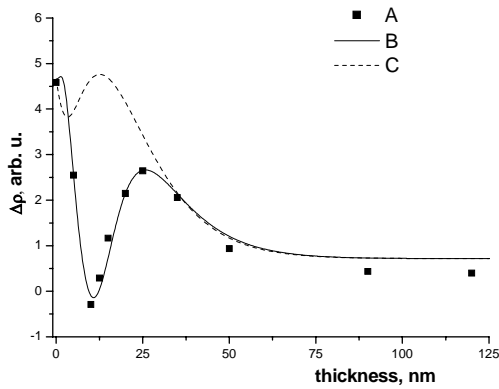


Fig. 6. The polarization difference $\Delta\rho$ as a function of the thickness of metal film on the TIR prism surface at an angle of light incidence $\phi_0 = 42^\circ < \phi_{cr}$: A – experiment; B (C) – calculations made with (without) allowance for optical constants dependence on the film thickness at the following parameter values: $n_0 = 1.4742$; $n_2 = 1.003$; $N_1 = n_1 + i\chi_1$; $n_1 = 0.2 + \exp(-0.2 - d/L)$; $\chi_1 = 3.6(1 - \exp(-d/L))$; $L = 11$ nm.

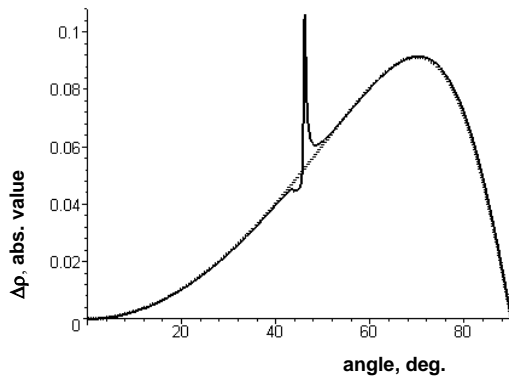


Fig. 7. The calculated dependences of polarization difference $\Delta\rho$ (full curve) and external Fresnel reflection (broken curve) on the angle of light incidence on the prism with a gold film 90 nm thick.

characterized by peak amplitude and angular position, and contains information on the real and imaginary parts of the refractive index of the sample under investigation. One can easily verify this by applying the traditional Fresnel equations for external reflection from a material with a complex refractive index. By varying the real and imaginary parts of the refractive index one can form, without SPR appearance, such characteristics which agree satisfactorily with the curves presented in Fig. 7 (at least in the curve pieces which vary monotonically). Their analysis could give some additional knowledge concerning relationship between the dielectric function and metal film thickness (this problem seems to deserve special consideration).

5. Conclusion

Let us note, first of all, that measurement of SPR with the PM technique makes it possible to get such characteristics of the effect that are more convenient for practical application. Contrary to the traditional measurements of the minimal signal in the extremum of angular dependence of SPR, the PM technique was used to measure the maximal signal. This was a rather serious reason for performance of our analysis and getting the results considered. This fact is of special importance when, due to some reasons, SPR effect appears as a small measurable signal. When measuring polarization difference $\Delta\rho$ in this case, nothing prevents signal amplification that is present at measurement of p -polarization only. Besides, a bigger, as compared to the traditional measuring procedure, signal value (as well as better signal-to-noise merit) improves the resolving power when determining the angle corresponding to the extreme value of the polarization difference. And knowledge of this value is related to increase of detectability of the corresponding facilities.

A discrepancy between the given characteristics that take or do not take into account the dependence of the dielectric function on the film thickness is observed in the whole angle range. The maximal quantitative distinction takes place below the critical angle (see Fig. 6). The agreement between the results of theoretical calculation and experimental data was obtained by using, as a preliminary model, an exponential dependence of the effective values of optical parameters on the metal film thickness, the characteristic length L being the only adjustable parameter. Its value (11 ± 0.5 nm) determined from the condition of best agreement between the calculated and experimental dependences remains the same for all angle values. It also agrees well with the results of other authors [18].

SPR registration with the PM technique has better detectability than the traditional procedures in what refers to revealing the features of SPR characteristics. This is due to the principle of physical differentiation of both (ρ_s and ρ_p) dependences measured with the PM technique. From an analysis of these characteristics it follows that there are components in the polarization difference of internal reflection, $\Delta\rho = \left(|R_s|^2 - |R_p|^2 \right)$,

that are not related to the resonance interaction. One of these components is related to attenuated TIR that is pronounced at small film thicknesses, while another is related to reflection from the surface of metal film when its thickness grows.

Acknowledgements

The authors are grateful to S.A. Zynyo for sample preparation and O.S. Lytvyn for AFM studies of the samples.

References

1. V.V. Mar'enko, S.N. Savenkov // *Optika i spektroskopiya* **78**, p. 614-616 (1995) (in Russian).
2. M. Born, E. Wolf, *Principles of Optics*. Cambridge University Press, Cambridge, 1999.
3. D. Roy // *Appl. Spectroscopy* **55**, p. 1046-1052 (2001).
4. Dhesingh Ravi Shankaran, K. Vengatajalabathy Gobi, Norio Miura // *Sensors and Actuators B: Chemical* **121**, p. 158-177 (2007).
5. *Surface Polaritons, Electromagnetic Waves at Surfaces and Interfaces*, Eds. V.M. Agranovich, D.L. Mills. North-Holland, Amsterdam and New York, 1982.
6. N.L. Dmitruk, V.G. Litovchenko, V.L. Strizhevsky, *Surface Polaritons in Semiconductors and Insulators*. Naukova Dumka, Kiev, 1989 (in Russian).
7. A. Otto // *Z. Physik* **216**, p. 398-410 (1968).
8. E. Kretschmann // *Z. Physik* **241**, p. 313-324 (1971).
9. E.F. Venger, I.E. Matyash, B.K. Serdega // *Optika i spektroskopiya* **94**, p. 33-37 (2003) (in Russian).
10. I.E. Matyash, B.K. Serdega // *Semiconductors* **38**, p. 657-662 (2004).
11. M. Cardona, *Modulation Spectroscopy*. Academic Press, New York, 1969.
12. S.V. Kondratenko, I.E. Matyash, B.K. Serdega // *Semiconductor Physics, Quantum Electronics & Optoelectronics* **7**, p. 195-198 (2004).
13. R.M.A. Azzam, N.M. Bashara, *Ellipsometry and Polarized Light*. North-Holland, Amsterdam, 1980.
14. *Patent Ukraine No. 20949*, Intern. Cl. G01N 21/55, A technique for measurement of the parameters of surface plasmon resonance, B.K. Serdega, L.J. Berzhinsky (2007).
15. S.N. Jaspersen, S.E. Schnatterly // *Rev. Sci. Instrum.* **40**, p. 761-767 (1969).
16. O.V. Rengevych, Yu.M. Shirshov, Yu.V. Ushenin, A.G. Beketov // *Semiconductor Physics, Quantum Electronics & Optoelectronics* **2**, p. 28-35 (1999).
17. H. Piller, Lead tin telluride, In: *Handbook of Optical Constants of Solids*, vol. 2, Ed. E.D. Palik. Academic Press, New York, 1991.
18. U. Kreibig, M. Vollmer, *Optical Properties of Metal Clusters* (Springer Series in Materials Science). Springer-Verlag, Berlin, 1995.